ELSEVIER

Chemical Physics 278 (2002) 101–110

Chemical Physics

www.elsevier.com/locate/chemphys

An ELF and AIM study of a model charge resonance complex: intermolecular interactions between two strong electron acceptors

D.B. Chesnut [a,*], L.J. Bartolotti [b]

[a] *Department of Chemistry, P.M. Gross Chemical Laboratory, Duke University, Durham, NC 27708, USA*
[b] *The North Carolina Supercomputing Center, Research Triangle Park, NC 27709, USA*

Received 29 October 2001

Abstract

Calculations at the B3LYP/6-31G(d,p)//B3LYP/6-31G(d,p) level involving the electron localization function (ELF) and atoms-in-molecules (AIM) methods have been carried out for the $(Li)_2$TCNE–quinone complex as a model of a charge resonance complex in the solid state. No intermolecular ELF basins were found but a small delocalization index of about one between the complex components in the ground singlet state is indicative of some electron pair sharing. Several unusual ELF topological features are observed which are interpreted in terms of the electronic structure of the model system.

Keywords: Atoms-in-molecules; Electron localization function; Delocalization index; Pair numbers; Basin populations; Charge resonance complexes

1. Introduction

In the 1960s there was much interest in the charge resonance complexes involving the strong electron acceptor tetracyanoquinodimethan, TCNQ, and tetracyanoethylene, TCNE (see Scheme 1). Of these two the complexes involving TCNQ were of greater interest because of their unusual structures and physical properties [1,2]. They exist as ion radical salts such as the 2:3 cesium salt, $(Cs^+)_2(TCNQ)_3^{-2}$ [3] and the 2:4 methyltriphenyl phosphonium and arsonium salts, $((\varphi)_3CH_3X^+)_2(TCNQ)_4^{-2}$ (with X = P, As) [4]. Many of the TCNQ compounds are semi-conductors and even semi-metallic, while some, such as the two salts mentioned above, possess low-lying triplet excited states and exhibit dense triplet exciton behavior. The dense triplet exciton solids are characterized by small singlet–triplet separations of the order of 1–10 kcal/mol. Groups of supermolecular TCNQ molecules act as single supermolecular species in this regard, a trimer of TCNQ molecules in the cesium salt and a tetramer in the arsonium and phosphonium salts. All these properties are thought to be due to the strong

* Corresponding author. Tel.: +1-919-660-1537; fax: +1-919-660-1605.
E-mail address: dbc@chem.duke.edu (D.B. Chesnut).

0301-0104/02/$ - see front matter
PII: S0301-0104(02)00378-6

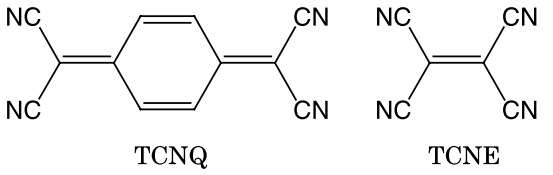

Scheme 1.

overlapping π systems; the stability of these systems is remarkable since the supermolecular species carry a net negative charge. In order to better understand the interaction of such systems we have investigated the energetics of some model charge resonance dimers and also atoms-in-molecules (AIM) [5,6] and electron localization function (ELF) [7–14] studies of a model TNCE–quinone dimeric complex.

2. Theoretical background

The two approaches we used here to characterize the nature of the bonding interactions are the *delocalization index* of Fradera et al. [5] based on the electron pair density in the AIM approach [6], and ELF isosurfaces and *bond basin populations* from the ELF approach of Becke and Edgecombe [7] as extensively developed by Savin and Silvi and coworkers [8–14]. In the AIM approach atomic basins are derived from the scalar field of the electron density, $\rho(\vec{r})$, while ELF basins arise from a potential (see below) which is based on strong physical arguments regarding the Fermi hole [15,16] and the corresponding tendency of electron pairs to occupy different regions of space.

ELF is a robust descriptor of chemical bonding based on topological analyses of local quantum mechanical functions related to the Pauli exclusion principle. For a closed shell single determinantal wavefunction built from Hartree–Fock or Kohn–Sham orbitals, φ_j, the ELF function of position $\eta = \eta(\vec{r})$ is *defined* as

$$\eta = \frac{1}{1 + \left(\frac{D}{D_h}\right)^2}, \tag{1}$$

where

$$D = \frac{1}{2}\sum_{j=1}^{N} |\nabla\varphi_j|^2 - \frac{1}{8}\frac{|\nabla\rho|^2}{\rho},$$
$$D_h = \frac{3}{10}(3\pi^2)^{2/3}\rho^{5/3}, \tag{2}$$
$$\rho = \sum_{j=1}^{N} |\varphi_j|^2,$$

and where the scaling factor is chosen to be the homogeneous electron gas kinetic energy density of a system of the same electron density. D is the local Pauli kinetic energy density, the excess kinetic energy electrons have (due to the Pauli exclusion principle) compared to a system of bosons of the same density [10]. The ELF function can be viewed as a local measure of the Pauli repulsion between electrons due to the exclusion principle and allows one to define regions of space that are associated with different electron pairs in a molecule or solid.

Using the vector field of the gradient of the electron localization function, the topology of the ELF function can be used to define basins within which one or more electron pairs are to be found [9–11,14]. Gradient paths end within each subsystem at what are called *attractors*. The region of three-dimensional space traversed by all gradient paths that terminate at a given attractor defines the *basin* of the attractor. ELF basins are labeled as either core or valence basins. Core basins contain a nucleus while valence basins do not; hydrogen basins are taken as exceptions since, although they contain a proton, they represent a shared pair interaction. A valence basin is characterized by its number of connections to core basins, referred to as its synaptic order. Basins are connected if they are bounded by part of a common surface.

The population of a basin Ω_i, N_i, is given by integrating the total electron density, $\rho(\vec{r})$, over the basin volume. The ELF basin populations are particularly

$$N_i = \int_{\Omega_i} \rho(\vec{r})\,\mathrm{d}\vec{r} \tag{3}$$

important in that they tend to reflect delocalization effects and, in the case of bond basins, the bond order.

Bader's AIM approach [6] is based on the electron density, $\rho(\vec{r})$, a key observable in a mol-

ecule's description. The gradient field of the electron density defines atomic basins which can be integrated over to obtain AIM atomic basin electron populations. The delocalization index is defined in terms of the electron pair density as it relates to the AIM atomic basins. The (spinless) electron pair density [15,16], $P_2(\vec{r_1},\vec{r_2})$, is the diagonal part of the reduced second order density matrix and is normalized as

$$\int \mathrm{d}\vec{r_1} \int \mathrm{d}\vec{r_2} P_2(\vec{r_1},\vec{r_2}) = \int \mathrm{d}\vec{r_1}(N-1)\rho(\vec{r_1}) = N(N-1), \tag{4}$$

where $\rho(\vec{r_1})$ is the electron number density and N the total number of electrons. It proves convenient to define the pair density in terms of a quantity explicitly referencing the antisymmetric character of electron wavefunctions,

$$P_2(\vec{r_1},\vec{r_2}) = \rho(\vec{r_1})\rho(\vec{r_2})[1+f(\vec{r_1},\vec{r_2})], \tag{5}$$

so that

$$\frac{P_2(\vec{r_1},\vec{r_2})}{\rho(\vec{r_2})} - \rho(\vec{r_1}) = \rho(\vec{r_1}) f(\vec{r_1},\vec{r_2}). \tag{6}$$

The quantity on the left is the *conditional probability* of finding an electron at $\vec{r_1}$ *given* that there is one at $\vec{r_2}$, minus the number density at $\vec{r_1}$, $\rho(\vec{r_1})$, where integration for the number density is over the coordinates of all electrons. This quantity (either side of Eq. (6)) is the *Fermi hole* [15,16] associated with the reference electron at $\vec{r_2}$.

If we integrate the pair density over two AIM basins, Ω_i and Ω_j, we obtain by definition the quantity N_{ij}, the interbasin pair number, and, using Eq. (5), one can write [6,17,18]

$$\begin{aligned} N_{ij} &= \int_{\Omega_i} \mathrm{d}\vec{r_1} \int_{\Omega_j} \mathrm{d}\vec{r_2} P_2(\vec{r_1},\vec{r_2}) \\ &= \int_{\Omega_i} \mathrm{d}\vec{r_1} \int_{\Omega_j} \mathrm{d}\vec{r_2} \rho(\vec{r_1})\rho(\vec{r_2})[1+f(\vec{r_1},\vec{r_2})] \\ &= N_i N_j + \int_{\Omega_i} \mathrm{d}\vec{r_1} \int_{\Omega_j} \mathrm{d}\vec{r_2} \rho(\vec{r_1})\rho(\vec{r_2}) f(\vec{r_1},\vec{r_2}) \\ &= N_i N_j - F_{ij}, \end{aligned} \tag{7}$$

where N_i and N_j are the basin populations (electron numbers) and where here, in contrast to Fradera et al. [5], we have explicitly introduced the negative sign in the definition of F_{ij} because it is generally positive.

It is the sum of the off-diagonal terms, $F_{ij}+F_{ji} = 2F_{ij} \equiv \delta_{ij}$, in the AIM approach that Fradera et al. [5] define as the *delocalization index* and use as a quantitative measure of the sharing of electrons between basins Ω_i and Ω_j; they also denote F_{ii} as the *atomic localization index*.

3. Theoretical details

The AIM and ELF calculations were carried out employing the TopMod Package of Noury and coworkers [19] in the B3LYP approach [20,21]. The same ELF formula was used for both open and closed shell systems. Step sizes of 0.2 a.u. and box sizes that extended 5.0 a.u. from the outermost atomic coordinates in each direction were typically used. The numerical uncertainty of the ELF basin populations calculated with a step size of 0.02 a.u. is expected to be of the order of 0.05.

The various dimeric structures employed here used optimized neutral and anionic monomer geometries found at the B3LYP and UB3LYP levels, respectively, with Gaussian 98 [22]. The dimers considered here are modeled on configurations found for several typical TCNQ salts [3,4] mentioned earlier where supermolecular n-mers ($n = 3, 4$) are formed.

The experimental dispositions of the TCNQ molecules within an n-mer (supermolecule) show both translated (Tr) and side-slipped (Ss) conformations as schematically shown in Scheme 2; the directly superimposed form (Su) is not found experimentally although we do carry out calculations on it in our study. The Tr forms are found *within* the strongly interacting n-mers, while the Ss configuration is found for those TCNQ molecules belonging to *adjacent* n-mers. In the (essentially isomorphous) arsonium and phosphonium salts [4] the molecular separation within the tetramer is approximately 3.20 Å, while between tetramers the separation is 3.58 Å. In the cesium salt, however, the same spacings are 3.22 and 3.26 Å [3].

Because the TCNQ dimers are very large, we have limited our ELF and AIM studies to the model TCNE–quinone dimer shown in Scheme 3

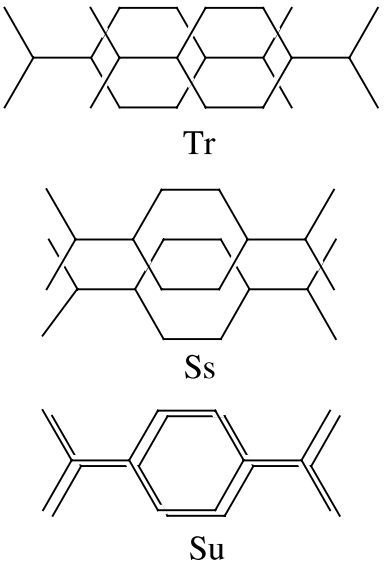

Scheme 2. Translated (Tr), side-slipped (Ss), and superimposed (Su) TCNQ structures.

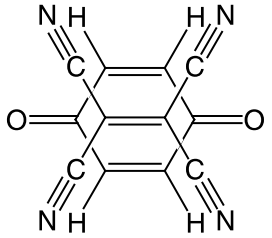

Scheme 3. The TCNE–quinone dimer.

in its superimposed configuration. Both TCNE and quinone are strong electron acceptors and in the superimposed configuration mimic the stable Tr structure found for the TCNQ *n*-mers which exhibit a bonds-over-bonds arrangement. In order to compare this case to the model TCNQ salts, an intermolecular separation of 3.20 Å was initially employed. The ELF and AIM studies were carried out on the minimum energy interplanar separation (3.444 Å) of the $(Li)_2$TCNE–quinone complex salt (vide infra). Dimers were studied with and without countercharges represented either as point charges or as first column atomic species. The mean distance between coordinating nitrogens and the cesium atoms in the cesium TCNQ salt [3] is 3.308 Å, and it is this distance that was used in the TCNQ and TCNE model systems.

3.1. Energies

3.1.1. TCNQ dimers

The physical systems we are attempting to model exist as solids. Our results must be examined in this regard since we are replacing the involved, many-molecule interactions in a complicated solid by relatively simple dimers. The extent to which the model is appropriate is to be judged on how well it tends to mimic the behavior of the real systems.

We examined TCNQ dimers as neutral species (using fixed neutral TCNQ monomer geometries) and as anionic species (using fixed TCNQ monomer anion geometries) both without and with compensating positive charges (point charges, q^{1+}, or hydrogen (H) or lithium (Li) atoms). When either no charges or point charges were employed, the charge on the TCNQ dimers was dictated by the neutral or anionic geometry used. In the H and Li cases the anionic TCNQ monomer geometries were employed but the overall molecular systems were treated as neutral; the gross Mulliken population data in Table 1 indicate that the lithium atom is essentially ionic but not so for hydrogen for reasons that we shall shortly discuss.

In Table 1 we observe that in all but the Li case the Tr structure is the lowest in energy among the singlet states and in the exceptional case is less than 2 kcal/mol above the ground singlet. The singlet–triplet separations are significantly reduced when anionic TCNQ species are involved except in the case of the hydrogen "salt". It seems clear physically that using the doubly negatively charged dimer by itself is not a good approach although the energies of this type of system tend to mimic the TCNQ salts in the solid in several other respects. Although we did not carry out any ELF studies generally on the TCNQ dimers, examination of the use of point charges in the TCNE–quinone system (vide infra) shows that significant charge is placed in the region of the positive point charges, a phenomenon we wish to avoid since we believe that in the solid state the species involved are basically ionic. It appears that the positive

Table 1
Relative energies (kcal/mol) for various TCNQ dimers in their translated (Tr), side-slipped (Ss), and superimposed (Su) configurations

	$^1E_{rel}$	$^3E - {}^1E$	Q_M
$(TCNQ^0)_2$			
Tr	0.0	29.54	
Ss	5.11	22.99	
Su	16.21	11.39	
$(TCNQ^-)_2$			
Tr	0.0	−0.76	
Ss	3.10	1.62	
Su	4.97	12.23	
$(q^{1+})_2(TCNQ^-)_2$			
Tr	0.0	−5.82	
Ss	4.25	−4.19	
Su	24.10	−8.47	
$(H)_2(TCNQ)_2$			
Tr	0.0	−61.99	0.12 (0.05)
Ss	5.45	−61.62	0.13 (0.05)
Su	18.31	−64.16	0.12 (0.05)
$(Li^{1+})_2(TCNQ^-)_2$			
Tr	1.63	0.63	0.83 (0.83)
Ss	0.0	3.24	0.83 (0.83)
Su	10.17	13.32	0.89 (0.89)

The first column of data presents the relative energies of the three singlet ground states, and the second column is the singlet–triplet splitting for each conformer. $(q^{1+})_2(TCNQ^-)_2$ is the dimer where unit point charges are used. Q_M is the Mulliken gross charge (ground singlet out of parentheses, excited triplet state in parentheses) at the H and Li nuclei.

point charges act as protons without any basis functions centered on them. The strong potential draws electron density away from the TCNQ moieties to the region of the positive point charges.

The result for the point charges case is not unexpected, and the results for the $(H)_2(TCNQ^-)_2$ compounds confirm this. In these cases the triplet states are strongly below the singlet parent and exhibit Mulliken gross charges at the H atoms that clearly indicate that each hydrogen loses little of its electron to the TCNQ dimer. On the other hand, for the $(Li^+)_2(TCNQ^-)_2$ case the Li Mulliken charges show the Li atom to basically be a cation with the TCNQ dimers containing nearly two full negative charges, a situation we *do* desire in our model. Essentially identical results are found when Na is used in place of Li. The different reaction of the systems to hydrogen, lithium, and sodium is clearly reflective of their relative electronegativities.

We conclude that the lithium salt would be a reasonable model for the TCNQ ion radical salts seen in the crystalline state.

3.1.2. TCNE–quinone

Table 2 shows data for the TCNE–quinone complexes at the same interplanar spacings of 3.20 Å as the systems in Table 1. All except the TCNE–quinone example used anionic monomer geometries. Again, for reasons given above, the point charge model and the hydrogen compound are clearly inappropriate models, while the Li, Na, and K salts produce results consistent with our understanding of the systems we wish to model: small singlet–triplet separations and structures where two cations are interacting with a doubly negatively charged dimer. As mentioned above, the ELF isosurfaces picture for the point charge model system clearly shows basins in the regions of the point charges containing about half an electron each. Because the Li, Na, and K salts behave essentially the same, and since Li has many fewer electrons, we have focused on the $(Li)_2$TCNE–quinone compound as our representative model.

We also investigated the energy dependence of $(Li)_2$TCNE–quinone as a function of the interplanar separation, R. In each case the TCNE and quinone molecules (with anionic monomer geometries) were kept superimposed as shown earlier, and the position of the Li atoms were determined

Table 2
Singlet–triplet splittings ($^3E_{rel} - {}^1E_{rel}$, kcal/mol) for the various dimers of TCNE and quinone with and without compensating charges in their superimposed configurations

Configuration	$^3E_{rel} - {}^1E_{rel}$	Q_M
(TCNE)quinone	45.01	–
$((TCNE^-)quinone^-)$	2.54	–
$(q^{1+})_2((TCNE^-)quinone^-)$	−6.86	–
$(H)_2$((TCNE)quinone)	−64.43	0.11 (0.05)
$(Li^{1+})_2((TCNE^-)quinone^-)$	6.56	0.95 (0.83)
$(Na^{1+})_2((TCNE^-)quinone^-)$	7.19	0.95 (0.88)
$(K^{1+})_2((TCNE^-)quinone^-)$	8.58	0.95 (0.95)

The Mulliken gross charge (Q_M, ground singlet out of parentheses, excited triplet state in parentheses) is given for the H, Li, Na, and K atoms.

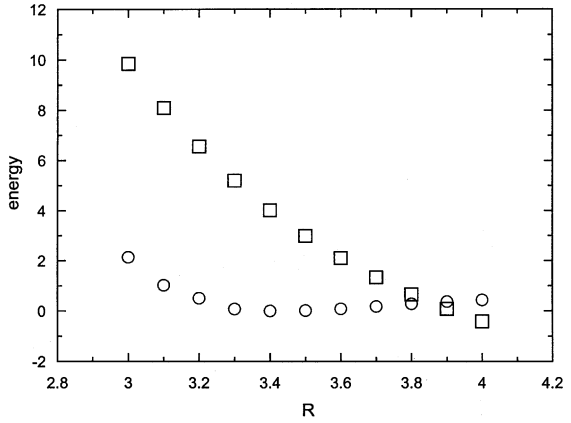

Fig. 1. Energies of the singlet state (circles, kcal/mol) of the $(Li)_2$TCNE–quinone complex relative to the minimum value at $R = 3.444$ Å and the singlet–triplet energy difference (squares, kcal/mol) as a function of the interplanar separation (R, Å).

by keeping the lithium–oxygen (on quinone) and the lithium–nitrogen (on TCNE) the same and equal to 3.308 Å. The results of this study are shown in Fig. 1 where the singlet state energies are plotted relative to the minimum energy (−844.09811 a.u. at $R = 3.444$ Å) along with the singlet–triplet separations, all in kcal/mol. The equilibrium structure is in a shallow and broad potential energy well, and we note that at values of R greater than 3.8 Å the triplet state becomes lower than its parent singlet.

This singlet–triplet crossing results in the interesting and not unexpected result that for $R = 3.9$ Å the B3LYP singlet energy wrongly converges to too high a value while the case for $R = 4.0$ Å is "normal". To obtain a value for the singlet state at $R = 3.9$ Å, the singlet energy curve was quadratically fit through its last three "good" points ($R = 3.7$, 3.8, and 4.0 Å) and a fit result used for the singlet energy for $R = 3.9$ Å. In so doing the singlet–triplet energy difference point at $R = 3.9$ Å falls nicely on the upper curve, indicating the validity of the procedure used. Identical results are obtained if one use the Gaussian keyword guess = mix which allows mixing of the HOMO and LUMO orbitals to avoid problems of near degeneracy.

For the subsequent AIM and ELF studies it is the $(Li)_2$TCNE–quinone complex at an intereplanar separation of 3.444 Å that is employed where the singlet–triplet energy separation is 3.54 kcal/mol.

The stability of $(Li)_2$TCNE–quinone at its equilibrium interplanar separation and fixed intramolecular geometries is shown by its energetics of formation shown below (kcal/mol) in Scheme 4 where TCNEan represents the TCNE anion and quinonean stands for the quinone anion. Being good electron acceptors, the energies of the isolated TCNQ and quinone molecules are lowered by becoming ion radicals (both LUMOs in the isolated neutral molecules are negative), but it is quite expensive due to the large ionization energy of lithium. Bringing the ions together to form the overall–neutral complex is exothermic due mainly to the coulomb energy recovered as well as a stabilizing interaction between the TCNE–quinone dimer pair.

The bonding situation in the $(Li)_2$TCNE–quinone complex is revealed by an examination of the ELF basin isosurfaces shown in Figs. 2(a) and (b) for $\eta = 0.85$ where the complex is viewed side-on (Fig. 2(a)) and from above and slightly to the front of the TCNE portion of the complex (Fig. 2(b)). The absence of any intermolecular attractors (and basins) in Fig. 2(a) clearly indicates that the complex is not stabilized by conventional strong covalent bonds between atoms in the different monomers. Fig. 2(b) shows that in the complex the TCNE and quinone entities (and, of course, the

$2Li$	=	$2Li^+ + 2e^-$	259.3
$TCNE + e^-$	=	TCNEan	−80.2
$Quinone + e^-$	=	quinonean	−50.0
$2Li + TCNE + quinone$	=	$2Li^+ + TCNEan + quinonean$	129.1
$2Li + TCNEan + quinonean$	=	$(Li)_2$TCNE–quinone	−195.1
$2Li^+ + TCNE + quinone$	=	$(Li)_2$TCNE–quinone	−66.1

Scheme 4.

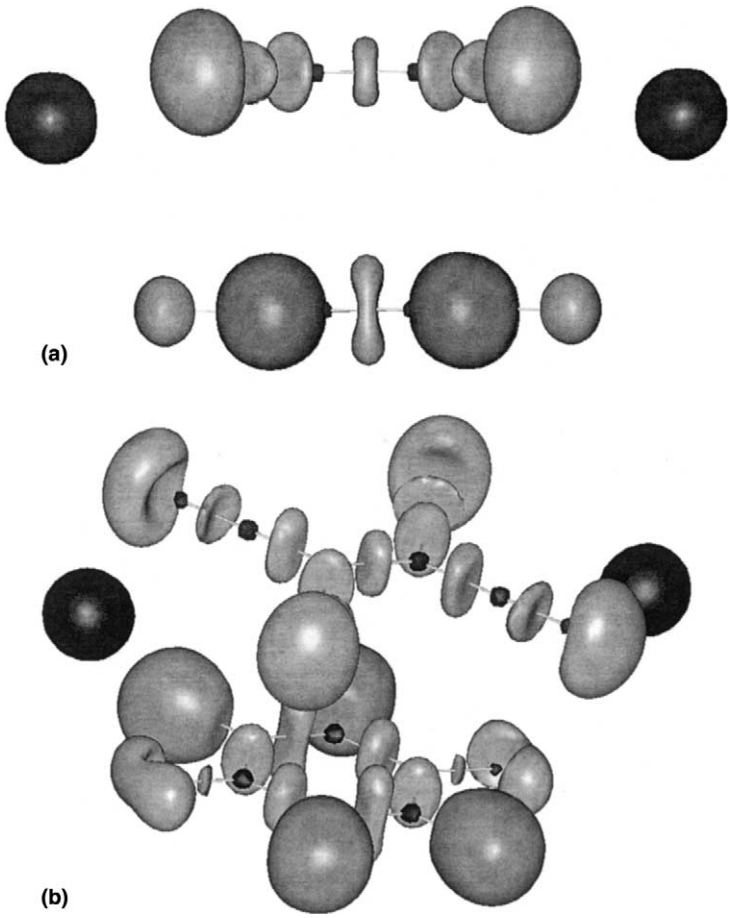

Fig. 2. ELF isosurfaces for $\eta = 0.85$ for the singlet ground state of $(Li)_2$TCNE–quinone viewing the system (a) from a side view and (b) from above and slightly to the front of the complex. In both cases the TCNE portion of the complex is at the top of the figure.

Li^+ ions) retain the basic character of their isolated species.

Table 3 contains the ELF basin populations for the non-equivalent basins, and one can see that the changes from the isolated ionic species are noticeable but small. (Note that in Tables 3 and 4 population sums are slightly less than the number of electrons involved; this is likely due to neglect of those regions of space where the density is less than 10^{-5} a.u.) In both singlet and (excited) triplet states, the Li exists essentially as the Li^+ cation, although the change in the triplet state of +0.11 electron is noted to which we return later. In the complex there is a transfer of about 0.5 electron from quinone to TCNE; in the triplet state TCNE has essentially an overall charge of −1, losing the extra 0.5 electron it possessed in the ground singlet state to both quinone and the Li atoms. This particular transfer of charge is confirmed in Table 4 by the AIM populations where almost identical figures are observed.

Table 5 contains the summed intermolecular and inter-ionic delocalization indices for the singlet and triplet state of the complex. The individual contributions to the overall TCNE–quinone delocalization index are all small, the largest being about 0.036; most of the larger contributions involve the quinone heavy atoms and the central, doubly bonded carbons in TCNE. But even though small individually, there

Table 3
Summary of ELF lone pair (lp) and bond basin populations (number of electrons) for the isolated TCNE, quinone, and Li ions, and population *changes* in these moieties in the $(Li)_2$TCNE–quinone complex

	TCNE anion	TCNE in $(Li)_2$TCNE–quinone	
		Singlet	Triplet
N(lp)	3.43	0.12	0.01
CN	4.26	−0.02	0.06
CC	2.42	−0.04	−0.07
C=C	2.20	−0.15	0.0
C=C(lp)[a]	0.76 (2)	0.23 (2)	0.03 (2)
Core	20.83	−0.04	−0.04
Total	64.96	0.48	0.03
	Quinone anion	Quinone in $(Li)_2$TCNE–quinone	
		Singlet	Triplet
O(lp)	5.64	−0.24	−0.24
CO	1.93	0.35	0.33
(O)CC	2.53	−0.20	−0.13
C=C	3.35	0.10 (2)	0.09
Core	25.01	−0.13	0.11
Total	56.96	−0.52	−0.27
	Li^+ ion	Li in $(Li)_2$TCNE–quinone	
		Singlet	Triplet
Total	(2.0)[b]	0.01	0.11 (2)
Grand totals	125.93	−0.02	−0.02

Total core populations are also given along with the overall totals. Numbers in parentheses indicate the population in each of several basins and are noted for those cases where multiple basins exist.

[a] Doubly bonded carbon "lone pair" basins located above and below each carbon atom.

[b] The isolated Li^+ cation.

Table 4
Summary of AIM atomic basin populations (number of electrons) for the isolated TCNE, quinone, and Li ions, and population *changes* in these moieties in the $(Li)_2$TCNE–quinone complex

	TCNE anion	TCNE in $(Li)_2$TCNE–quinone	
		Singlet	Triplet
N	8.16	0.10	0.02
C(N)	5.18	0.02	0.03
C	5.79	−0.02	−0.08
Total	64.93	0.47	0.06
	Quinone anion	Quinone in $(Li)_2$TCNE–quinone	
		Singlet	Triplet
O	9.12	0.08	0.12
C(O)	5.20	−0.22	−0.19
C	6.08	−0.02	0.00
H	0.99	−0.04	−0.03
Total	56.94	−0.53	−0.29
	Li^+ ion	Li in $(Li)_2$TCNE–quinone	
		Singlet	Triplets
Total	(2.0)[a]	0.02	0.11
Grand totals	125.87	−0.01	−0.01

[a] The isolated Li^+ cation.

Table 5
Summed intermolecular and inter-ionic delocalization indices for the singlet and triplet states of $(Li)_2$TCNE–quinone

	TCNE–quinone	TCNE–Li^+	Quinone–Li^+
Singlet	0.97	0.08	0.02
Triplet	0.27	0.04	0.27

are many contributions because of the stacked form of the dimer. In the ground singlet state they sum to 0.97 which is of the order of what one would expect for a single covalent bond [5]. The individual contributions are not large enough to give rise to ELF bond basins, but collectively they do provide a stabilizing interaction for the complex.

There are two other features of the ELF basin isosurfaces that call for comment and interpretation. As one lowers η to a value of about 0.15 for the excited triplet state, a new surface appears around each Li atom at a distance of 1.59 Å from the Li core attractor; see Fig. 3. This is the lithium valence basin (the 2s shell) holding the slight excess of charge on lithium that is not accommodated in the core basin (1s shell); here the core population is 2.02 while that of the valence basin is 0.09. The distance of 1.59 Å of this basin from the Li core is almost precisely what one expects for the 2s radius of maximum charge density in the lithium atom [23]. No such effect is seen for the singlet ground state since in that case the 2s valence basin of Li is essentially empty.

The second feature of the complex basin worth noting are two small basins above and below the

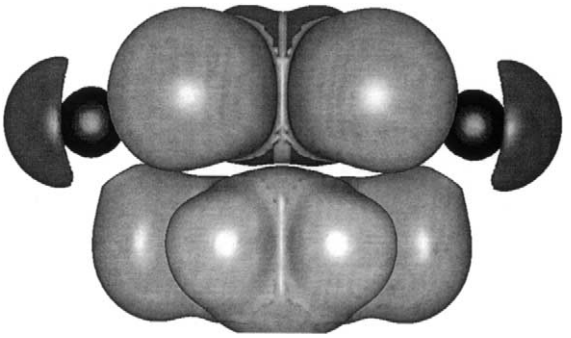

Fig. 3. Side view of the ELF isosurfaces for $\eta = 0.03$ for the excited triplet state of $(Li)_2$TCNE–quinone showing the partially filled 2s valence basins about each Li atom. The TCNE portion of the complex is at the top of the figure.

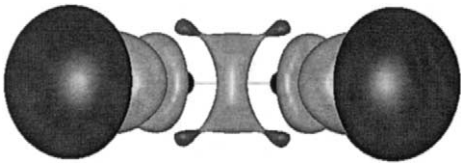

Fig. 4. A side view of the $\eta = 0.75$ isosurfaces for the TCNE anion radical showing the unusual non-bonding basins above and below the core basins of each of the central formally doubly bonded carbon atoms.

formally double bonded carbon atoms in the TCNE part of the complex that are present in addition to a carbon–carbon bond basin (between the two carbon atoms). Fig. 4 exhibits these basins in the case of the TCNE anion radical. These unusual basins are present in both singlet and triplet states and also are seen in the isolated TCNE ion radical; they are *not* seen in the isolated neutral TCNE molecule. We ascribe these basins to the antibonding character of the neutral TCNE LUMO (and the highest occupied alpha orbital in the UB3LYP state of the ion radical).

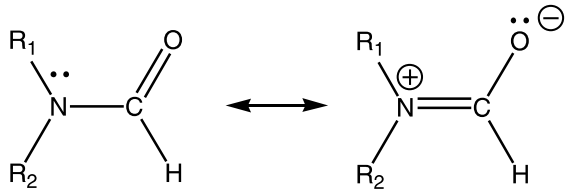

Scheme 5.

The C=C bond lengthens considerably upon formation of the TCNE ion radical from neutral TCNE, being 1.373 Å in the neutral species and 1.442 Å in the anion radical. The "extra" basins are a distance of 0.79 Å essentially vertically above and below each carbon, a distance one associates with a lone or non-bonding pair of electrons [24]. In cases of the amide bond [25] and in the trans-bent HSiSiH molecule [26] similar basins appear and are considered to be associated with lone pair character on the nitrogen and silicon atoms, respectively. In the case of amides one pictures the resonance interaction to be as in Scheme 5 and in the ELF representation small basins are seen above and below the nitrogen core. There are no such lone pairs in the TCNE ion radical; furthermore, the integrated spin density in these extra basins is only 7.1% of the total density (for the planar $H_2C{=}CH_2$ ion radical the percentage is only 6.2%), so one cannot argue that we are seeing the "unpaired" electron itself in the antibonding orbital. Since a π antibonding orbital will tend to provide ionic structures involving the antibonded atoms, we conclude that these unusual basins must represent a contribution of polar lone pair resonance structures to the overall electronic picture of the molecule (see Scheme 6).

This effect is unusual and likely deserves further study.

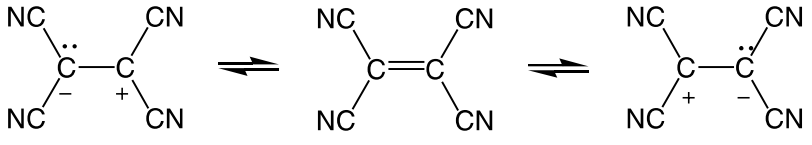

Scheme 6. Polar and neutral contributions to the electronic structure of the TCNE ion radical about the central CC bond.

Acknowledgements

We are indebted to the North Carolina Supercomputing Center for providing CPU time on the IBM SP and SGI Origin 2000 platforms that allowed these calculations to be carried out.

References

[1] J.C. Bailey, D.B. Chesnut, J. Chem. Phys. 51 (1969) 5118, and references therein.
[2] D.B. Chesnut, in: S.S. Eaton, G.R. Eaton, K. Salikhov, Foundations of Modern EPR, World Scientific Publishing, River Edge, NJ, pp. 512–521.
[3] C.J. Fritchie, P. Arthur Jr., Acta Cryst. 21 (1966) 139.
[4] A.T. McPhail, G.M. Semeniuk, D.B. Chesnut, J. Chem. Soc. A 1971 (1971) 2174.
[5] X. Fradera, M.A. Austen, R.F.W. Bader, J. Phys. Chem. A 103 (1999) 304.
[6] R.F. Bader, Atoms in Molecules: A Quantum Theory, Oxford University Press, Oxford, 1994.
[7] A.D. Becke, K.E. Edgecombe, J. Chem. Phys. 92 (1990) 5397.
[8] A. Savin, A.D. Becke, J. Flad, R. Nesper, H. Preuss, H.G. von Schnering, Angew. Chem. Int. Ed. Engl. 30 (1991) 409.
[9] B. Silvi, A. Savin, Nature 371 (1994) 683.
[10] A. Savin, B. Silvi, F. Colonna, Can. J. Chem. 74 (1996) 1088.
[11] M. Kohout, A. Savin, Int. J. Quantum Chem. 60 (1996) 875.
[12] A. Savin, R. Nesper, S. Wengert, T. Fässler, Angew. Chem. Int. Ed. Engl. 36 (1997) 1809.
[13] D. Marx, A. Savin, Angew. Chem. Int. Ed. Engl. 36 (1997) 2077.
[14] S. Noury, F. Colonna, A. Savin, B. Silvi, J. Mol. Struct. 450 (1998) 59.
[15] R. McWeeny, Rev. Mod. Phys. 32 (1960) 335.
[16] R. McWeeny, Methods of Molecular Quantum Mechanics, second ed., Academic Press, New York, 1989.
[17] R.F.W. Bader, M.E. Stephens, Chem. Phys. Lett. 26 (1974) 445.
[18] R.F.W. Bader, M.E. Stephens, J. Am. Chem. Soc. 97 (1975) 7391.
[19] S. Noury, X. Krokidis, F. Fuster, B. Silvi, Comput. Chem. 23 (1999) 597.
[20] A.D. Becke, J. Chem. Phys. 98 (1993) 5648.
[21] C. Lee, W. Yang, R.G. Paar, Phys. Rev. B 37 (1988) 785.
[22] M.J. Frisch et al., Gaussian 98, Revision A.7, Gaussian, Inc., Pittsburgh, PA, 1998.
[23] J.C. Slater, in: Quantum Theory of Matter, second ed., McGraw-Hill, New York, 1968, p. 150.
[24] D.B. Chesnut, J. Phys. Chem. A 104 (2000) 11644.
[25] D.B. Chesnut, J. Phys. Chem. A 104 (2000) 7635.
[26] D.B. Chesnut, Heteroatom Chem. 13 (2002) 53.